Regulation of COX-2 Expression and IL-6 Release by Particulate Matter in Airway Epithelial Cells

Yutong Zhao[1], Peter V. Usatyuk[1], Irina A. Gorshkova[1], Donghong He[1], Ting Wang[1], Liliana Moreno-Vinasco[1], Alison S. Geyh[2], Patrick N. Breysse[2], Jonathan M. Samet[3], Ernst Wm. Spannhake[2], Joe G. N. Garcia[1], and Viswanathan Natarajan[1]

[1]Department of Medicine, University of Chicago, Chicago, Illinois; [2]Department of Environmental Health Sciences, and [3]Department of Epidemiology, Bloomberg School of Public Health, Johns Hopkins University, Baltimore, Maryland

Particulate matter (PM) in ambient air is a risk factor for human respiratory and cardiovascular diseases. The delivery of PM to airway epithelial cells has been linked to release of proinflammatory cytokines; however, the mechanisms of PM-induced inflammatory responses are not well-characterized. This study demonstrates that PM induces cyclooxygenase (COX)-2 expression and IL-6 release through both a reactive oxygen species (ROS)-dependent NF-κB pathway and an ROS-independent C/EBPβ pathway in human bronchial epithelial cells (HBEpCs) in culture. Treatment of HBEpCs with Baltimore PM induced ROS production, COX-2 expression, and IL-6 release. Pretreatment with N-acetylcysteine (NAC) or EUK-134, in a dose-dependent manner, attenuated PM-induced ROS production, COX-2 expression, and IL-6 release. The PM-induced ROS was significantly of mitochondrial origin, as evidenced by increased oxidation of the mitochondrially targeted hydroethidine to hydroxyethidium by reaction with superoxide. Exposure of HBEpCs to PM stimulated phosphorylation of NF-κB and C/EBPβ, while the NF-κB inhibitor, Bay11–7082, or C/EBPβ siRNA attenuated PM-induced COX-2 expression and IL-6 release. Furthermore, NAC or EUK-134 attenuated PM-induced activation of NF-κB; however, NAC or EUK-134 had no effect on phosphorylation of C/EBPβ. In addition, inhibition of COX-2 partly attenuated PM-induced Prostaglandin E2 and IL-6 release.

Keywords: ambient particulate matter; cytokine; reactive oxygen species; transcriptional factors; airway epithelium

CLINICAL RELEVANCE

Particulate matter (PM) is a risk factor for human respiratory and cardiovascular diseases. Mechanisms linking PM-induced cyclooxygenase-2 expression and IL-6 secretion via mitochondrial reactive oxygen species (ROS)-dependent and ROS-independent pathways are provided.

Recent epidemiologic studies have linked short-term exposure to ambient particulate matter (PM) with increased morbidity and mortality associated with cardiovascular and cardiopulmonary illnesses such as myocardial infarction, congestive heart failure, asthma, and bronchitis (1–4).The assessment of the health effects of PM is challenging because the chemical and physical properties of PM vary greatly with time, region, meteorology, and source category (5–9). Furthermore, sex, age, and pre-existing health conditions seem to influence the morbidity and mortality associated with acute exposure to PM (10). However, mechanism(s) of PM-induced exacerbations of cardiopulmonary diseases are not yet well characterized. Rodents and airway epithelial cells have been widely used as model systems to better understand the pathophysiology of acute exposure of PM in exacerbation of cardiovascular/cardiopulmonary diseases (7, 8, 11–13). In vivo exposure of rodents to PM

increases secretion of cytokines/chemokines (such as IL-1β, IL-6, IL-8, and TNF-α), generation of reactive oxygen species, and infiltration of neutrophils; induces airway hyperresponsiveness to acetylcholine; and compromises host defense, leading to lung injury and inflammation (9, 14–20). While impaired host defense may arise from enhanced apoptosis of alveolar macrophages and decreased phagocytosis, inflammation seems to result from elevated cytokines/chemokines production in airway epithelial, endothelial, and Th1/Th2 lymphocytes. In vitro, exposure of alveolar macrophages, epithelial cells, neutrophils, and dendritic cells to PM stimulates ROS production and cytokine/chemokine secretion, which are consistent with findings of in vivo studies (7, 9, 13, 17, 21). In vivo, among the various cytokines, secretion of IL-6 from the lung is significantly higher in response to environmental toxins and stimuli, including PM (9, 16, 19). Exposure of healthy people and individuals with coronary artery disease to PM increases IL-6 levels in the serum (22), while elevated IL-6 level in the circulation is linked to cardiovascular dysfunction (23–26). A recent study in mice suggests that PM accelerates arterial thrombosis via an IL-6–dependent mechanism, linking PM exposure to thrombosis (19). IL-6 is a pleotropic cytokine that is involved in proinflammatory, antiinflammatory, and proliferative responses in lung (22, 27, 28), where different cell types, including alveolar macrophages, epithelial cells, endothelial cells, lymphocytes, and dendritic cells, secrete IL-6 (21, 29–34). A variety of stimuli enhances IL-6 production via transcriptional regulation of the IL-6 gene by NF-κB, AP1, MRE, and C/EBPβ regulatory elements (34, 35). Activation of NF-κB by PM and residual oil fly ash induces IL-6 gene expression in the human airway epithelial cell line, BEAS-2B (7, 14), and generation of ROS is associated with PM-induced NF-κB activation (36–38).

In developing a human bronchial epithelial cell model to study the biochemical and toxicologic effects of PM exposure, we observed that PM less than 10 μM in aerodynamic diameter collected from Baltimore ambient air elicited increased ROS generation and IL-6 production in primary cultures of human bronchial epithelial cells (HBEpCs). As molecular mechanisms linking PM-induced ROS generation to transcriptional regulation of IL-6 gene expression and secretion have not been well characterized, we hypothesized that ROS may provide a link as an intracellular signal, generated in response to PM, in transcriptional regulation of IL-6 secretion in HBEpCs. Here we provide evidence for a novel pathway that involves COX-2

signaling in IL-6 secretion through ROS-dependent and ROS-independent pathways in HBEpCs. Furthermore, our results show the participation of mitochondrial electron transport, but not NADPH oxidase, in PM-induced ROS production in these cells.

MATERIALS AND METHODS

Materials

N-acetylcysteine (NAC) was purchased from Sigma-Aldrich (St. Louis, MO). C/EBPβ siRNA and antibodies to phospho-JNK1/2, JNK1, NF-κB (RelA), and C/EBPβ were from Santa Cruz Biotechnology, Inc. (Santa Cruz, CA). Antibodies to phospho-C/EBPβ and phospho-IκB (ser 32) were procured from Cell Signaling Technology (Beverly, MA). Scrambled siRNA was from Dharmacon (Chicago, IL). Mito-hydroethidine (MitoSOX Red), Dihydroethidium (hydroethidine), 6-carboxy-2′,7′-dichlorodihydrofluorescein diacetate (DCFDA), Mito Tracker, and Alexa Fluor 488 rabbit secondary antibody were purchased from Molecular Probes (Eugene, OR). Transmembrane Transfection reagent was from Qiagen (Valencia, CA). EUK-134, NS-398, prostaglandin (PG)E2, and antibodies for COX-1 and COX-2 were from Cayman Chemical, Inc. (Ann Arbor, MI). DCFDA Horseradish peroxidase–conjugated goat anti-rabbit and anti-mouse second antibodies were purchased from Molecular Probes (Eugene, OR). Rotenone, stigmatellin, and apocynin were procured from Sigma. The ECL kit for detection of proteins by Western blotting was obtained from Amersham Pharmacia, Inc. (Piscataway, NJ). The EIA kit for PGE2 measurement and antibodies for COX-1 and COX-2 were from Cayman Chemical, Inc. (Ann Arbor, MI). All other reagents were of analytical grade.

Collection and Characterization of PM

The cyclone used for collection of ambient PM in Baltimore, MD was a commercially available unit (model HVS3; CS3, Inc., Sandpoint, ID), which was designed to collect PM as a part of vacuum carpet dust sampler for lead and pesticide analysis (39). We have used this cyclone for PM collection in previous studies of ambient PM toxicity (40, 41). The cyclone collector has a theoretical particle size cut point (D50) of 0.8 μm when operated at 1 m³/minute. The sampling pump used for the system is a BRL-3300M (HI-Q Environmental, San Diego, CA), commonly used for high-volume environmental sampling. Analysis for elemental metals content was conducted by high-resolution ICP-MS. Sample preparation and analysis were performed at the Lamont-Doherty Earth Observatory, Columbia University. Sample digestion was conducted in a Milestone MEGA microwave digestion oven (Model Mega MLS 1200; Milestone, Italy). Nitric acid and hydrofluoric acid used for sample digestion were Optima Grade (Fisher Scientific, Columbia, MD). Ultra-high-purity water (Millipore, Billerica, MA) and Teflon round bottom vials (Savillex, Minnetonka, MN) were used for all sample digestion processes. Before digestion, the sample was added to a Teflon vial along with 20 μl ethanol, 60 μl ultrapure water, and 225 μl nitric acid. The vial was sealed and placed in a Teflon microwave digestion bomb containing 10 ml 65% nitric acid to ensure uniform heating. Samples were then irradiated in two steps under an identical four-phase power cycle. After step 1, 40 μl concentrated hydrofluoric acid were added to the vial. Once step 2 was completed, the digests were diluted with 5 ml ultrapure water, and 1% or 2% nitric acid to achieve a final acid concentration of approximately 4% nitric acid and 0.8% hydrofluoric acid. Samples were sonicated for 20 minutes and the membrane was removed. Fifteen to twenty percent of digests in each digest batch were procedural blanks (acids only). Field blanks were treated as samples, and samples and procedural blanks from digestion batches were analyzed on the same day. Data were collected for all isotopes of interest at the appropriate resolving power (RP) to avoid isobaric interferences. Be, Ag, Cd, Sn, Sb, Cs, La, Pt, Tl, and Pb, for which interferences are not a problem, were run at RP 400; Na, Mg, Al, S, Ca, Sc, Ti, V, Cr, Mn, Fe, Co, Ni, Cu, Zn at RP of 3,000 to 4,300; and K, As, and Se at RP greater than or equal to 9,300. Indium was added to all samples, blanks, and standards as an internal drift corrector and run in all resolving powers. Quantification was done by external and internal standardization, and data were drift-corrected using indium. The output was converted to a mass value and

blank corrected. Samples that were below the limit of detection based on daily procedural blanks were flagged. Indium-corrected elemental sensitivities in either matrix normally differed by less than 5% sample for all elements. The metal content of the PM used in the present study, derived from the digestion of 0.328 mg of sample, is presented in Table 1.

Cell Culture

Primary human bronchial epithelial cells were isolated from normal human lung obtained from lung transplant donors following typical procedures as previously described (42–44). The isolated P_0 HBEpCs were then seeded, at a density of 1.5×10^4 cells/cm², onto T-75 flasks in Basal Essential Basal Medium (BEBM; Lonza, Walkersville, MD) that was serum free, and supplemented with growth factors. Cells were incubated at 37°C in 5% CO_2 and 95% air to approximately 80% confluence and subsequently propagated in 6-well plates. All experiments were performed between passages 1 and 4.

Treatment of Cell Cultures with PM

PM was added to BEBM to produce a stock PM suspension at a concentration of 1.0 mg/ml. After sonication in a water bath for 2 minutes and shaking at room temperature for 1 hour, BEBM or BEBM containing PM was added to the surfaces of the cultures. After incubation for the prescribed period, the medium was removed from the surfaces of the cultures for analysis by enzyme-linked immunosorbent assay (ELISA), and protein was extracted from the underlying cells, as described. The dose of PM used ranged from 10 to 100 μg/ml. After incubation for the indicated time period, the medium was removed from the cultures for analysis of cytokines by ELISA, and total protein content was determined from the cell lysates using a Pierce protein assay kit (Pierce Chemical Co., Rockford, IL). Using estimates of normal breathing volumes over a 24-hour period and airway surface area, these doses range from 20 to 200 times the amount of PM predicted to deposit on epithelial surfaces during exposures to PM less than 10 microns in aerodynamic diameter (PM_{10}) at the National Ambient Air Quality Standard level of 150 μg/m³. This may represent an overestimation of dose in that it assumes that none of the size fractions of the PM remain in suspension in the overlaying 1.0 ml of medium and that the entire dose deposits on the surfaces of the cell cultures during the treatment period.

Preparation of Cell Lysates and Western Blotting

After indicated treatments, HBEpCs were rinsed twice with ice-cold PBS and lysed in 200 μl of lysis buffer containing 20 mM Tris-HCl (pH 7.4), 150 mM NaCl, 2 mM EGTA, 5 mM β-glycerophosphate, 1 mM $MgCl_2$, 1% Triton X-100, 1 mM sodium orthovanadate, 10 μg/ml protease inhibitors, 1 μg/ml aprotinin, 1 μg/ml leupeptin, and 1 μg/ml pepstatin. Cell lysates were incubated at 4°C for 15 minutes, sonicated on ice for 15 seconds, and centrifuged at $5,000 \times g$ for 5 minutes at 4°C. Protein concentration was determined with a BCA protein assay kit (Pierce) using bovine serum albumin (BSA) as standard. Equal amounts of protein (20 μg) were subjected to 10% SDS/PAGE gels, transferred to polyvinylidene difluoride membranes, blocked with 5% (wt/vol) BSA in TBST (25 mM Tris-HCl, pH 7.4, 137 mM NaCl and

TABLE 1. METAL CONTENT OF BALTIMORE PARTICULATE MATTER

Metal	μg/g	Metal	μg/g	Metal	μg/g
Be 9	0.6	Cr 52	326.0	Sr 88	110.8
Na 23	6222.4	Mn 55	2133.9	Ag 109	1.7
Mg 25	10750.1	Fe 57	28273.9	Cd 111	2.1
Al 27	12439.7	Co 59	9.7	Sn 118	20.8
S 34	6122.7	Ni 60	59.6	Sb 121	15.8
K 39	5824.3	Cu 63	2329.5	Cs 133	0.7
Ca 43	39619.8	Zn 66	645.6	La 139	21.3
Sc 45	3.3	As 75	4.3	Pb 204	119.7
Ti 47	2135.2	Se 78	7.4	Tl 205	0.3
V 51	76.3	Sr 86	111.0	Pb 208	122.1

0.1% Tween 20) for 1 hour, and incubated with primary antibodies in 5% (wt/vol) BSA in TBST for 1 hour at room temperature. The membranes were washed at least three times with TBST at 15-minute intervals and then incubated with either mouse or rabbit horseradish peroxidase–conjugated secondary antibody (1:3,000 dilution) for 1 to 2 hours at room temperature. The membranes were developed with an enhanced chemiluminescence detection system according to the manufacturer's instructions.

Transfection of Small Interfering RNA of C/EBPβ

HBEpCs (P1 or P2) were cultured onto 6-well plates. At 50 to 60% confluence, transient transfection of small interfering (si)RNA was performed using Transmessenger Transfection Reagent (Qiagen, Chatsworth, CA). Briefly, siRNA (50 nM) was condensed with Enhancer R and formulated with Transmessenger reagent, according to the manufacturer's instructions. The transfection complex was diluted in 900 μl of BEBM medium and added directly to the cells. The medium was replaced with complete BEGM medium after 3 hours. Cells were analyzed at 72 hours after transfection by Western blotting (44).

ROS Detection and Quantification in Cells by Epifluorescence Microscopy

PM-induced formation of ROS was quantified by fluorescence microscopy (45, 46). HBEpCs ($\sim$ 80% confluent) in chamber slides or glass-bottom 35-mm dishes were loaded with DCFDA (10 μM) in EBM-2 basal medium for 30 minutes at 37°C in a 95% air, 5% CO_2 environment. After 30 minutes of loading, the medium containing DCFDA was aspirated and the cells were rinsed once with BEBM medium, then preincubated with agents for the indicated time periods, followed by exposure to PM. At the end of the incubation, the cells were examined under a Nikon Eclipse TE 2000-S fluorescence microscope (Nikon, Tokyo, Japan) with a Hamamatsu digital CCD camera (Hamamatsu, Iwata, Japan), using a ×20 or ×60 objective lens and MetaVue software (Molecular Devices, Downingtown, PA).

Mitochondrial Superoxide Generation

PM-induced mitochondrial superoxide ($O_2^{\cdot-}$) production was quantified by MitoSOX Red, a redox-sensitive dye composed of hydroethidine linked to hexyl carbon chain to triphenylphosphonium group to target mitochondrial matrix because of the negative membrane potential across inner mitochondrial membrane. HBEpCs ($\sim$ 90% confluence) grown on glass-bottom 35-mm dishes were rinsed with BEBM, then challenged with vehicle or vehicle plus Baltimore PM (100 μg/ml). Then cells were loaded with MitoSOX Red (1 μM) for 10 minutes, washed, and used for imaging using immunofluorescence microscopy (47).

Measurement of IL-6 Secretion

HBEpCs grown on 6-well plates were challenged with PM for the indicated times and media were collected and centrifuged at 5,000 × *g* for 10 minutes at 4°C. The supernatants were transferred to new Eppendorf tubes and frozen at −80°C for later analysis of IL-6 with IL-6 ELISA kit according to the manufacturer's instructions.

Immunocytochemistry

HBEpCs grown on coverslips to approximately 80% confluence were challenged with LPA (1 μM) for 15 minutes. Coverslips were rinsed with PBS and treated with 3.7% formaldehyde in PBS at room temperature for 20 minutes. After washing with PBS, coverslips were incubated in blocking buffer (1% BSA in TBST) for 1 hour, and cells were subjected to immunostaining with antibody to NF-κB (RelA) (1:200 dilution) for 1 hour and washed four times with TBST followed by staining with a secondary antibody with Alexa Fluor 488 (1:200 dilution in blocking buffer) for 1 hour. After washing four times with TBST, the coverslips were mounted using commercial mounting medium for fluorescent microscopy (Kirkegaard and Perry Laboratories, Gaithersburg, MD) and were examined by immunofluorescent microscope with Hamamatsu digital camera using a ×60 oil immersion objective and MetaVue software.

Statistical Analyses

All results were subjected to statistical analysis using one-way ANOVA and, where appropriate, analyzed by Student–Newman-Keuls test. Data are expressed as means ± SD of triplicate samples from at least three independent experiments, and level of significance was taken as $P < 0.05$.

RESULTS

Inflammatory Cytokine Production by Baltimore PM in HBEpCs

An important function of airway epithelial cells is the ability to secrete proinflammatory cytokines in response to inhaled particles, allergens, and other environmental pollutants. To determine the ability of Baltimore PM to stimulate release of proinflammatory cytokines, we investigated HBEpCs grown under submerged or air–liquid interface (ALI) conditions. Consistent with earlier studies from PM collected from different locations (9), Baltimore PM (100 μg/ml, 24 h) stimulated GM-CSF, IL-1β, IL-6, and IL-8 secretion in submerged HBEpCs; however, cells grown under ALI showed significant stimulation of IL-6, but not GM-CSF, IL-1β, or IL-8 (Figures 1A and 1B). Furthermore, over 95% of PM-induced IL-6 was secreted toward the apical side of ALI cells with no significant change in the basolateral side of the ALI cells (data not shown). As our results show that Baltimore PM stimulated IL-6, but not GM-CSF, IL-1β, or IL-8, and that the magnitude of IL-6 produced after exposure to PM was very similar, if not identical, between the submerged and ALI cells, all further experiments were performed with primary HBEpCs grown under submerged conditions. The Baltimore PM–induced IL-6 secretion was dose dependent, which was statistically significant at 10, 50, and 100 μg/ml of PM exposure for 24 hours (Figure 2A). Interestingly, exposure of cells to Baltimore PM (100 μg/ml) did not stimulate IL-6 production at 6 hours; however, a significant release of IL-6
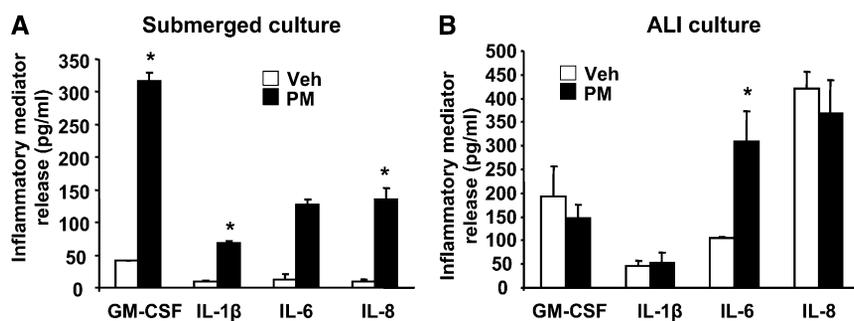
Figure 1. Inflammatory cytokine production by Baltimore particulate matter (PM) in submerged and air–liquid interface grown human bronchial epithelial cells (HBEpCs). HBEpCs grown (*A*) submerged or (*B*) at air-liquid interface were challenged with Baltimore PM (100 μg/ml) for 24 hours. Media were collected and centrifuged at 2,000 × *g* at 4°C, and cytokine levels were quantified by enzyme-linked immunosorbent assay (ELISA). Values are mean ± SD of three independent determinations in triplicate and expressed as picograms of cytokine released per milligram of protein in cell lysates. *Significantly different from cells exposed to vehicle alone (*P* < 0.05).
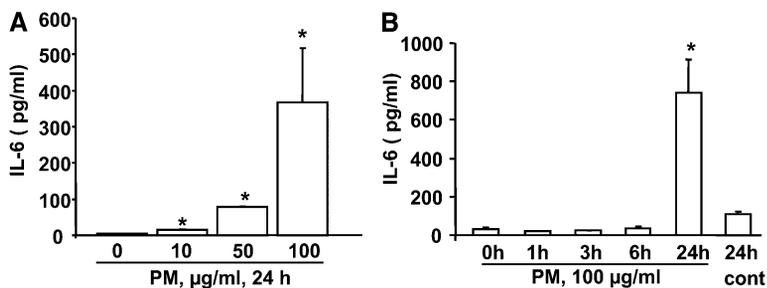
Figure 2. Dose- and Time-dependent release of IL-6 by Baltimore PM. HBEpCs grown to approximately 90% confluence were exposed to (*A*) varying concentrations or (*B*) different time periods with 100 µg/ml of Baltimore PM. At the end of the experiment, media were collected, centrifuged to remove any floating cells, and analyzed for IL-6 release by ELISA. Values are mean ± SD of at least three independent experiments. *Significantly different from cells exposed to 0 hours ($P < 0.05$).

was observed at 24 hours of PM exposure (Figure 2B). Measurement of lactate dehydrogenase in the medium revealed no significant difference between control cells and cells treated with PM (100 µg/ml) for 24 hours (vehicle, 22.5% of total LDH; PM, 24.6% of total LDH), suggesting that the Baltimore PM, under the experimental conditions, exhibited minimal cytotoxicity.
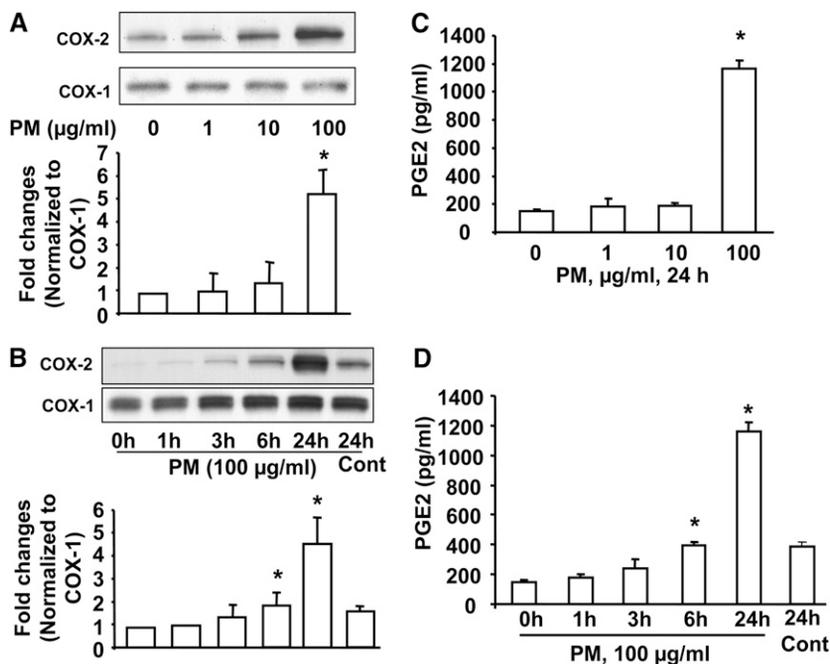
PM Induces COX-2 Expression and PGE2 Release in HBEpCs

The expression of COX-2 is up-regulated by inflammatory stimuli, and it has been reported that incinerator fly ash enhances liberation of arachidonic acid and expression of COX-2 in human airway epithelial cells (48) and RAW264.7 macrophages (49). As Baltimore PM induces IL-6 in HBEpCs, we evaluated the effect of Baltimore PM on COX-2 expression and PGE2 release. Exposure of HBEpCs to Baltimore PM resulted in an induction of COX-2, but not COX-1 (Figures 3A and 3B). In HBEpCs, COX-2 expression, compared with COX-1, was much lower under basal nonstimulatory condition, whereas an increase in COX-2 expression was seen at 6 and 24 hours of exposure to Baltimore PM. The induction of COX-2 expression was followed by an increased secretion of PGE2 (Figures 3C and 3D). These results demonstrate that Baltimore PM induces COX-2 expression and PGE2 release in HBEpCs.

### Mitochondria as a Source of PM-Induced ROS/$O_2^{.-}$ in HBEpCs

Previous studies indicate that exposure of alveolar macrophages and epithelial cells to PM produces large quantities of ROS (7,

13, 50); however, the exact source of ROS is poorly defined. Further, the ROS generated by environmental particulate pollutants may function as intra- and/or extracellular signaling molecule involved in cellular functions such as cytokine release and apoptosis. Therefore, we examined the effect of Baltimore PM on ROS generation in HBEpCs. Exposure of HBEpCs to Baltimore PM (100 µg/ml) enhanced ROS production in a time-dependent manner (Figure 4A), as measured by DCFDA oxidation. Further, an increase in hydrogen peroxide levels was also observed with exposure to PM (Figure 4B), suggesting enhanced ROS production and release into the medium. Next, we addressed the potential source of ROS generation by PM using the mitochondrial $O_2^{.-}$ indicator MitoSOx Red (47), and specific inhibitors of mitochondrial electron transport and NADPH-oxidase (51, 52). Exposure of HBEpCs, loaded with MitoSOX Red, to Baltimore PM for varying time periods resulted in enhanced oxidation of MitoSOX Red to 2-hydroxyethidine, which gave a strong orange fluorescence because of binding to mitochondrial DNA (Figure 4C). The oxidation of MitoSOX by Baltimore PM was time-dependent, with a 3-fold increase in fluorescence at 60 minutes of PM challenge (Figures 4C and 4D). The involvement of mitochondrial electron transport in PM-induced ROS generation was investigated using rotenone and stigmatellin. HBEpCs were pretreated with rotenone or stigmatellin before PM challenge. As shown in Figure 5A, rotenone and stigmatellin (blockers of state 1 and 3 of mitochondrial electron transport, respectively) significantly at-

Figure 3. Baltimore PM induces cyclooxygenase (COX)-2 expression and prostaglandin (PG)E2 release. In *A* and *C*, HBEpCs grown to approximately 90% confluence were treated with varying concentrations of Baltimore PM (1, 10, and 100 µg/ml) for 24 hours. (*A*) Cell lysates (20 µg proteins) were subjected to SDS-PAGE and Western blotted with anti–COX-1 and –COX-2 antibodies. Shown are representative blots from three independent experiments. Quantitative analyses from three independent experiments (mean ± SD). *$P < 0.05$ versus vehicle. (*C*) Total PGE2 released in the medium was quantified by ELISA. Values are mean ± SD of three independent experiments in triplicate and expressed as pg of PGE2/ml of medium. *Significantly different from vehicle-treated cells ($P < 0.01$). In *B* and *D*, HBEpCs ($\sim$ 90% confluence) were exposed to Baltimore PM (100 µg/ml) for 1, 3, 6, and 24 hours. At each time point, media were collected and cell lysates were prepared. (*B*) Cell lysates (20 µg proteins) were subjected to SDS-PAGE and Western blotted for COX-1 and COX-2. Shown are representative blots from three independent experiments. Quantitative analyses from three independent experiments (mean ± SD). *$P < 0.05$ versus 0 hours. (*D*) Media from the various time points were analyzed for PGE2 release by ELISA. Values are mean ± SD of

three independent experiments in triplicate and expressed as pg of PGE2/ml of medium. *Significantly different from vehicle-treated cells ($P < 0.01$).
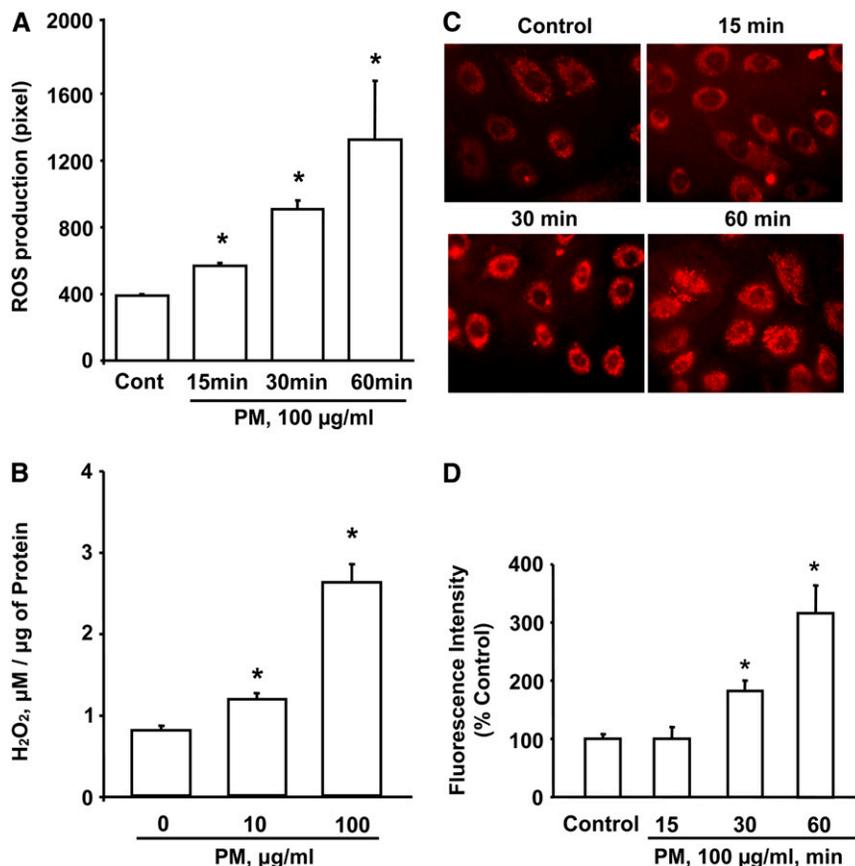
Figure 4. Baltimore PM induces reactive oxygen species (ROS) generation in HBEpCs. (*A*) HBEpCs grown on glass bottom-dishes to approximately 90% confluence were loaded with 10 μM DCFDA for 30 minutes. Cells were rinsed in basal medium without growth factors and exposed to Baltimore PM (100 μg/ml) for 15, 30, and 60 minutes. At the end of exposure, ROS formation was visualized under fluorescence microscope and quantified using image analysis. (*B*) HBEpCs grown on 35-mm dishes to approximately 90% confluence were challenged with 10 or 100 μg/ml of Baltimore PM for 60 minutes. Media were collected and H_2O_2 levels were measured using the Amplex Red assay. Values are mean $\pm$ SD of three experiments. *Significantly different from cells exposed to vehicle alone ($P < 0.05$). (*C*) HBEpCs grown on glass-bottom dishes to approximately 90% confluence, challenged with Baltimore PM (100 μg/ml) for 15, 30, and 60 minutes. At the end of each time point, cells were washed with EBM phenol red free media and were loaded with MitoSOX (1 μM) for 10 minutes. Cells were washed three times with EBM phenol red free media and intracellular MitoSOX Red-emitted fluorescence was visualized by immunofluorescence microscopy. (*D*) Intracellular MitoSOX Red-emitted fluorescence of *C* quantified by image analysis using MetaVue software. Values are mean $\pm$ SD of three independent experiments. *Significantly different from cells exposed to vehicle ($P < 0.05$).

tenuated Baltimore PM–induced ROS production. However, apocynin, which blocks flavin-containing enzyme(s), had no effect on PM-mediated DCFDA oxidation (Figure 5A). Analysis of DCFDA oxidation in living cells by immunofluorescence microscopy revealed that oxidation of DCFDA co-localized with Mito Tracker, a marker for mitochondria (Figure 5B) and pretreatment of cells with rotenone or stigmatellin, but not apocynin, attenuated the colocalization (*yellow*) of DCFDA oxidation (*green*) with fluorescence of Mito Tracker (*red*) (Figure

5B). These results support the role of mitochondrial electron transport, but not NADPH oxidase, in PM-induced ROS/O_2^- production in HBEpCs.

N-Acetylcysteine and EUK-134 Attenuate PM-Induced ROS Generation, COX-2 Expression, and IL-6 Secretion in HBEpCs

To elucidate the putative role of PM-induced ROS in COX-2 expression and IL-6 secretion, we pretreated cells with varying concentration of antioxidants, N-acetylcysteine (NAC), or
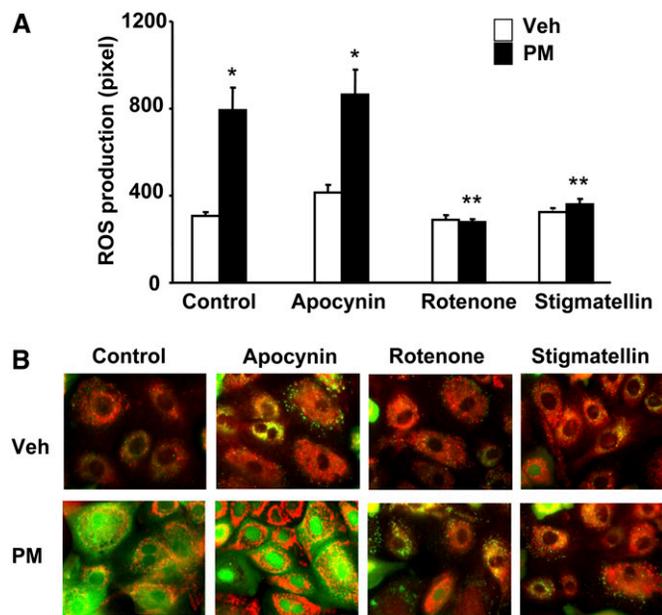
Figure 5. PM-induced ROS generation is dependent on mitochondrial electron transport. (*A*) HBEpCs grown to approximately 90% confluence were pretreated with apocynin (50 μM) or rotenone (2 μM) or stigmatellin (1 μM) for 1 hour before loading with 10 μM DCFDA for 30 minutes. Cells were rinsed and challenged with vehicle or vehicle plus Baltimore PM (100 μg/ml) for 30 minutes. Formation of ROS was quantified by immunofluorescence microscopy. Values are mean $\pm$ SD of three independent experiments. *Significantly different from cells exposed to vehicle ($P < 0.05$); **significantly different from cells challenged with Baltimore PM ($P < 0.01$). (*B*) HBEpCs grown on glass coverslips to approximately 90% confluence were pretreated with apocynin (50 μM), rotenone (2 μM), or stigmatellin (1 μM) for 1 hour before loading with 10 μM DCFDA and 50 nM Mito Tracker for 30 minutes. Cells were challenged with vehicle or vehicle plus Baltimore PM (100 μg/ml) for 30 minutes, and cells were visualized for ROS generation (*green*) and Mito Tracker (*red*) marker using fluorescence microscope. Co-localization of ROS (*green*) in mitochondria with Mito Tracker (*red*) is shown as *yellow*. Shown is a representative immunofluorescence micrograph from three independent experiments.

EUK-134 before challenge with PM (100 μg/ml). NAC (0.5 and 5 mM) or EUK-134 (5 and 25 μM) attenuated PM-induced DCFDA oxidation (Figures 6A and 6D), COX-2 expression (Figures 6B and 6E), and IL-6 production (Figures 6C and 6F) in HBEpCs. These data suggest the involvement ROS/cellular thiol redox status in PM-induced COX-2 expression and IL-6 secretion in HBEpCs.

PM Induces COX-2 Expression and IL-6 Secretion via NF-κB

As NF-κB is a key transcriptional activator of COX-2 and IL-6 genes (53, 54), we investigated the role of NF-κB in PM-induced COX-2 expression and IL-6 generation. Exposure of HBEpCs to Baltimore PM (100 μg/ml) for 15 minutes increased IκB phosphorylation, and translocation of NF-κB to the nucleus (Figures 7A and 7B). To study the role of NF-κB, cells were treated with the IκB kinase inhibitor, Bay11–7082 (1 and 5 μM). Bay11–7082 blocked PM-induced translocation of NF-κB to the nucleus (Figure 7B), COX-2 protein expression (Figure 7C), and IL-6 secretion (Figure 7D). These results suggest that PM-induced activation of NF-κB partly regulates COX-2 expression and IL-6 secretion in HBEpCs.

PM-Induced NF-κB Activation Is Attenuated by NAC and EUK-134

To determine the role of ROS in PM-induced NF-κB activation, we studied the effect of NAC and EUK-134 on IκB phosphorylation. As shown in Figures 8A and 8B, NAC (0.5 and 5.0 mM) or EUK-135 (5 μM) pretreatment for 1 hour attenuated PM-induced IκB phosphorylation. Further, pretreatment with NAC (5 mM) blocked PM-induced translocation of NF-κB to the nucleus of HBEpCs (Figure 8C). These results show that ROS generated by PM stimulate NF-κB activation in HBEpCs.

C/EBPβ Regulates PM-Induced COX-2 Expression and IL-6 Secretion via ROS-Independent Pathway

Our results with NAC and EUK-134 suggest a role for ROS-dependent activation of NF-κB in PM-induced COX-2 expression and IL-6 secretion. However, NAC and EUK-134 did not completely block either COX-2 expression or IL-6 production mediated by Baltimore PM, suggesting the involvement of other signaling pathways independent of ROS in COX-2 expression and IL-6 secretion in HBEpCs. As C/EBPβ is another transcriptional regulator of COX-2 and IL-6, we investigated the role of C/EBPβ in PM-induced COX-2 and IL-6 in HBEpCs. As shown in Figures 9A and 9B, PM exposure (100 μg/ml) for 15 minutes increased serine phosphorylation of C/EBPβ, which was not blocked by NAC (0.05–5.0 mM) or EUK-134 (5 μM), suggesting ROS-independent activation. To further establish the involvement of C/EBPβ in COX-2 expression and IL-6 secretion, we used C/EBPβ siRNA to knockdown C/EBPβ (Figure 9C). The effect of C/EBPβ siRNA was specific, as it had no effect on the protein expression of actin or ERK (results not shown). Knockdown of C/EBPβ blocked PM-mediated COX-2 expression (∼ 50% compared with scrambled siRNA plus PM) (Figure 9C) and IL-6 secretion (∼ 45% compared with scrambled siRNA plus PM) (Figure 9D). These results indicate the involvement of an ROS-independent pathway in PM-induced C/EBPβ activation and regulation of COX-2 and IL-6 in HBEpCs.

## Involvement of COX-2 and PGE2 in PM-Induced IL-6 Secretion in HBEpCs

To further determine the role of COX-2 in Baltimore PM-induced IL-6 secretion, HBEpCs were transfected with COX-2 siRNA (100 nM) for 72 hours or treated with NS-398 (50 μM),

an inhibitor of COX-2, for 1 hour before challenge with PM (100 μg/ml). The efficacy of the siRNA employed was determined by Western blotting for the protein expression of COX-2. As shown in Figure 10A, transfection of cells with siRNA for COX-2 blocked the expression of COX-2 without affecting COX-1 level, indicating a high degree of specificity. Furthermore, the PM-induced IL-6 secretion was attenuated by COX-2 siRNA (∼ 50% inhibition) (Figure 10B) and NS-398 (∼ 60% inhibition) (Figure 10C). Induction of COX-2 results in conversion of AA to PGE2 and PGD2 in mammalian cells. Having established a role for COX-2 in PM-mediated IL-6 release, we next determined if PGE2 is involved in IL-6 secretion via PGE2 receptors. Exposure of HBEpCs to PGE2 (10 and 100 ng/ml) for 24 hours resulted in increased IL-6 production (Figure 10D), suggesting PGE2-dependent IL-6 production. These results show a role for COX-2-mediated and PGE2-dependent production of IL-6 in HBEpCs.

DISCUSSION

The data presented in this study demonstrate that PM-induces IL-6 secretion in primary human airway epithelial cells and that this secretion is mediated through ROS-dependent activation of NF-κB/COX-2/PGE2 and ROS-independent activation of C/EBPβ/COX-2/PGE2 signaling pathways. Further, evidence is provided for the participation of the mitochondrial electron transport chain, but not NADPH oxidase, in Baltimore PM–induced ROS generation. Our finding that PM-induces IL-6 secretion via ROS-dependent and ROS-independent activation of COX-2/PGE2 pathways implies a novel signaling mechanism linking air pollution particles to the inflammatory response in the epithelium (Figure 11).

IL-6 is a multifunctional cytokine that is central to innate and acquired immune responses. In the airway, epithelial cells secrete IL-6 as a primary response to an external stimulus or as a secondary response to inflammatory mediators such as TNF-α or IL-1β (14, 15, 17, 27, 28). The increases in IL-6 levels observed in this study with Baltimore PM are similar to those described earlier using ROFA collected from the cyclone of a power plant in Florida (14); however, they differ from those described using ambient $PM_{2.5}$ collected from Cache Valley locations in Utah (20). The earlier studies were performed in the BEAS-2B transformed cell line (14), whereas primary cultures of HBEpCs were employed in the present investigation. ROFA stimulated IL-6/IL-8 gene expressions; however, in that study IL-6 secretion was not measured (14). Secretion of IL-6 in BEAS-2B cells exposed to $PM_{2.5}$ from Cache Valley, Utah was approximately 1.3- to 1.5-fold higher compared with control cells (20), while the Baltimore PM–induced IL-6 secretion in HBEpCs was at least 4- to 5-fold higher (Figure 2). This variation in IL-6 secretion between Cache Valley PM and Baltimore PM could be due to differences in the particle size, variation in particle composition, time, and collection location. It appears that the size of the particle PM from Baltimore versus $PM_{2.5}$ from Utah may contribute to the observed differences in IL-6 secretion. Endotoxin is a natural constituent of PM, which may contribute to the cytokine production in the epithelium (55); however, pretreatment of Baltimore PM with polymyxin B had no appreciable effect on IL-6 secretion (data not shown), suggesting no significant role of endotoxins as a contaminant in IL-6 production. In addition to IL-6, PM_{10} (EHC-93), obtained from the Environmental Health Directorate, Health Canada (Ottawa, ON, Canada) induced mRNA and protein expression of LIF, an IL-6–related glycoprotein, in HBEpCs (56). Similar to Baltimore PM, exposure of HBEpCs
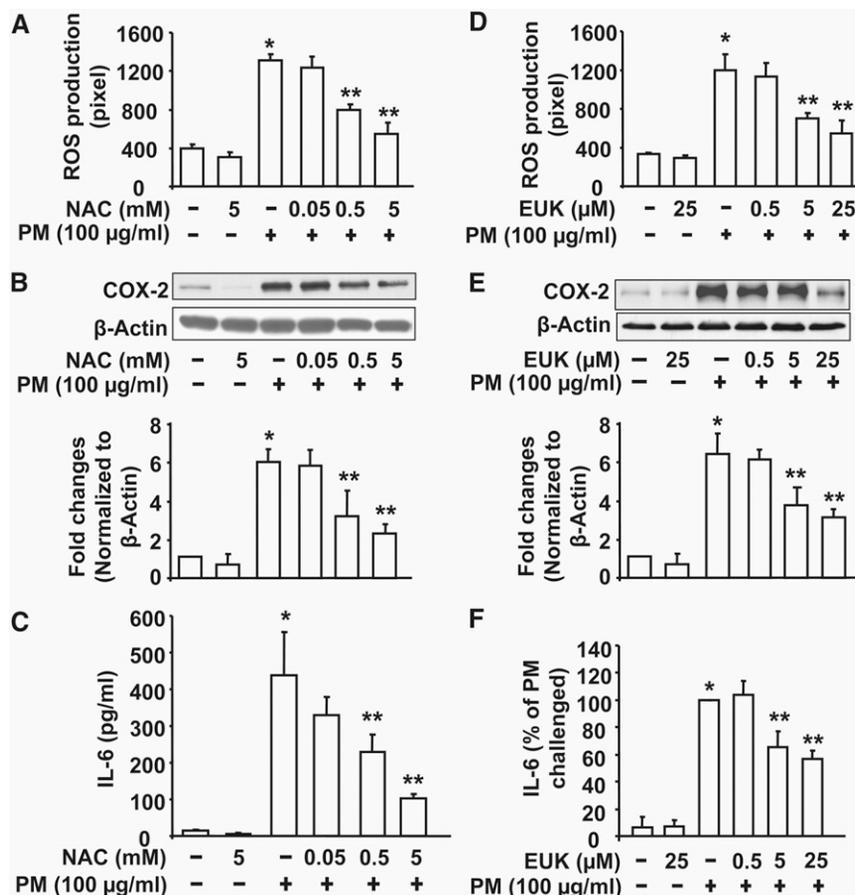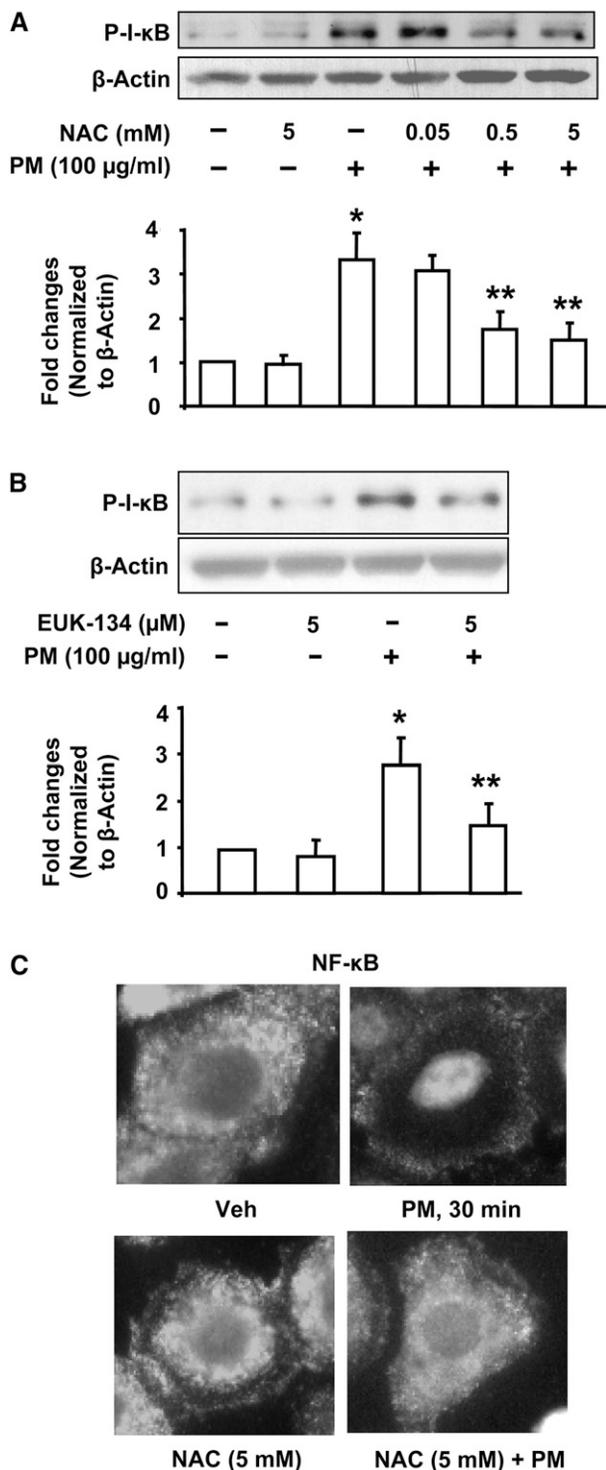
Figure 6. N-Acetylcysteine and EUK-134 attenuate Baltimore PM–induced ROS generation, COX-2 expression, and IL-6 secretion. HBEpCs grown in 35-mm dishes to approximately 90% confluence were pretreated with varying concentrations of N-acetylcysteine (NAC) (0.05, 0.5, and 5 mM) or EUK-134 (0.5, 5, and 25 μM) for 1 hour. In *A* and *D*, cells were loaded with 10 μM DCFDA for 30 minutes before addition of Baltimore PM (100 μg/ml) and ROS generation was quantified after 60 minutes using immunofluorescence microscopy. Values are mean $\pm$ SD of three independent experiments. *Significantly different from cells treated with vehicle ($P < 0.01$); **significantly different from cells exposed to Baltimore PM ($P < 0.05$). In *B* and *E*, cells after pretreatment with vehicle or NAC or EUK-134 were challenged with Baltimore PM (100 μM) for 24 hours, and cell lysates (20 μg proteins) were subjected to SDS-PAGE and Western blotted with anti–COX-2 and actin antibodies. Shown are representative blots from three independent experiments. Quantitative analyses from three independent experiments (mean $\pm$ SD). *$P < 0.05$ versus vehicle; **$P < 0.05$ versus PM challenge. In *C* and *F*, media were collected from cells (*B* and *E*), and analyzed for IL-6 by ELISA. Values are mean $\pm$ SD from three independent experiments in triplicate and represented as pg/ml of medium. *Significantly different from vehicle treated cells ($P < 0.05$); **significantly different from cells challenged with Baltimore PM ($P < 0.001$).
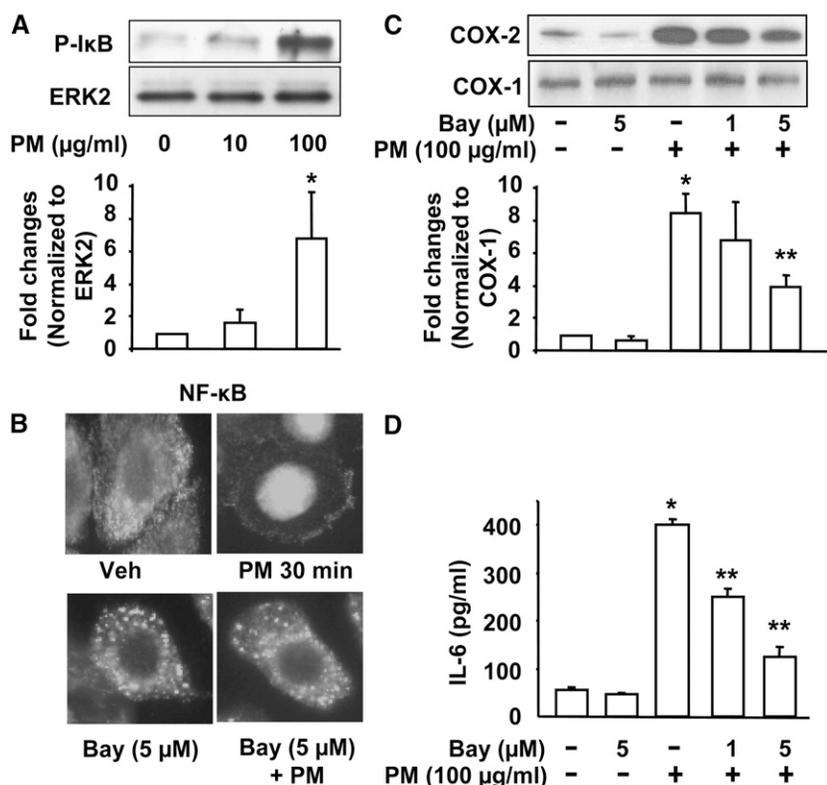
Figure 7. Baltimore PM-induced COX-2 expression and IL-6 secretion via NF-κB. In *A*, HBEpCs grown in 35-mm dishes to approximately 95% confluence were starved in basal EBM medium without any growth factors for 3 hours, and then challenged with Baltimore PM (10 and 100 μg/ml) for 15 minutes. Cell lysates (20 μg proteins) were subjected to SDS-PAGE and Western blotted with phospho-IkB and ERK2 antibodies. Shown are representative blots and quantitative analyses from three independent experiments (mean $\pm$ SD). *$P < 0.05$ versus vehicle. **$P < 0.05$ versus PM challenge. In *B*, HBEpCs in glass coverslips ($\sim$ 95% confluence) were pretreated with Bay compound (5 μM) for 60 minutes, cells were challenged with vehicle or vehicle plus Baltimore PM (100 μg/ml) for 15 minutes. Cells were washed, fixed, permeabilized, probed with anti-p65 antibody, and examined by immunofluorescence microscopy using a $\times$60 oil objective. Shown is a representative image from several independent experiments. In *C*, HBEpCs grown on 35-mm dishes were pretreated with varying concentrations of Bay compound (1 and 5 μM) for 60 minutes. Cells were challenged with vehicle or vehicle plus Baltimore PM (100 μg/ml) for 24 hours, cell lysates (20 μg proteins) were subjected to SDS-PAGE, and Western blotted with anti–COX-2 and actin antibodies. Shown are representative blots and quantitative analyses from three independent experiments (mean $\pm$ SD). *$P < 0.05$ versus vehicle; **$P < 0.05$ versus PM challenge. In *D*, media from *C* were analyzed by ELISA for IL-6. Values are mean $\pm$ SD from three independent experiments in triplicate. *Significantly different from cells exposed to vehicle ($P < 0.01$); **significantly different from cells exposed to Baltimore PM ($P < 0.05$).

Figure 8. N-Acetylcysteine and EUK-134 attenuate Baltimore PM-induced NF-κB activation. HBEpCs grown in 35-mm dishes to approximately 90% confluence were pretreated with varying concentrations of N-acetylcysteine (NAC) (0.05, 0.5, and 5 mM) or EUK-134 (5 μM) for 1 hour. In *A* and *B*, cells were challenged with vehicle or vehicle plus Baltimore PM (100 μg/ml) for 15 minutes, and cell lysates (20 μg proteins) were subjected to SDS-PAGE and Western blotted with anti–phospho-IkB and actin antibodies. Shown are representative blots and quantitative analyses from three independent experiments (mean ± SD). *$P < 0.05$ versus vehicle; **$P < 0.05$ versus PM challenge. In *C*, HBEpCs grown on glass coverslips (∼ 95% confluence) were pretreated with NAC (5 mM) for 60 minutes, cells were challenged with vehicle or vehicle plus Baltimore PM (100 μg/ml) for 15 minutes, and cells were washed, fixed, permeabilized, probed with anti-p65 antibody, and examined by immunofluorescence microscopy using a ×60 oil objective. Shown is a representative image from several independent experiments.

shown to control ROFA-induced IL-6 expression in cells of the BEAS-2B line (14). The results from this study show that Baltimore PM–induced IL-6 secretion is dependent on NF-κB, in that blocking NF-κB activation with Bay 117082 antagonized PM-induced IkB phosphorylation and IL-6 secretion. Further, the PM-induced NF-κB activation and IL-6 secretion were attenuated by NAC, suggesting a link between ROS generation to NF-κB activation and IL-6 expression. Although an earlier study with ROFA suggests a potential link between ROS and IL-6 expression in BEAS-2B cell line (14), the current study establishes a direct link between PM-dependent ROS generation in NF-κB activation and IL-6 secretion in primary HBEpCs. It has been shown that redox-active transition metals, redox-cycling quinones, and polycyclic aromatic hydrocarbons present in diesel exhaust particles (DEP) and PM generates ROS and oxygen free radicals in cultured macrophages, epithelial cells, and suspensions (13, 17). The source of ROS after exposure to DEP or PM is unclear, but may involve activation of NADPH oxidase (50) and/or leak from the mitochondrial electron transport chain (50, 57–59). In the present study, we have demonstrated that the mitochondrial inhibitors stigmatellin and rotenone, but not apocynin, attenuated Baltimore PM–stimulated ROS production, suggesting participation of the mitochondrial electron transport chain at complex I and III as the major source of ROS. While the nature of the redox-active metal(s) present in Baltimore PM that induces ROS production in primary HBEpCs has not been established, earlier studies indicate that vanadium present in ROFA may mediate ROS production (50), cytokine gene expression, and airway epithelial injury (60). Analyses of the Baltimore PM revealed the presence of vanadium (Table 1).

In addition to NF-κB, our results show a regulatory role for COX-2 in PM-induced IL-6 secretion in HBEpCs, as evidenced by COX-2 siRNA and COX-2 inhibitor studies. In accordance with the human COX-2 promoter having two NF-κB–binding sites, blocking NF-κB with Bay compound attenuated PM-mediated IL-6 secretion in HBEpCs. Interestingly, we have identified ROS-dependent and ROS-independent mechanisms of COX-2 expression in HBEpCs, demonstrating multiple signaling pathways of IL-6 regulation by PM. The ROS-dependent stimulation of COX-2 expression is via transcriptional regulation by NF-κB, while the ROS-independent expression of COX-2 requires activation of C/EBPβ in HBEpCs (Figure 9). Induction of COX-2 results in subsequent production of PGE2, and in the present study we show that exposure of HBEpCs to PM stimulated PGE2 secretion. Further, exogenous addition of
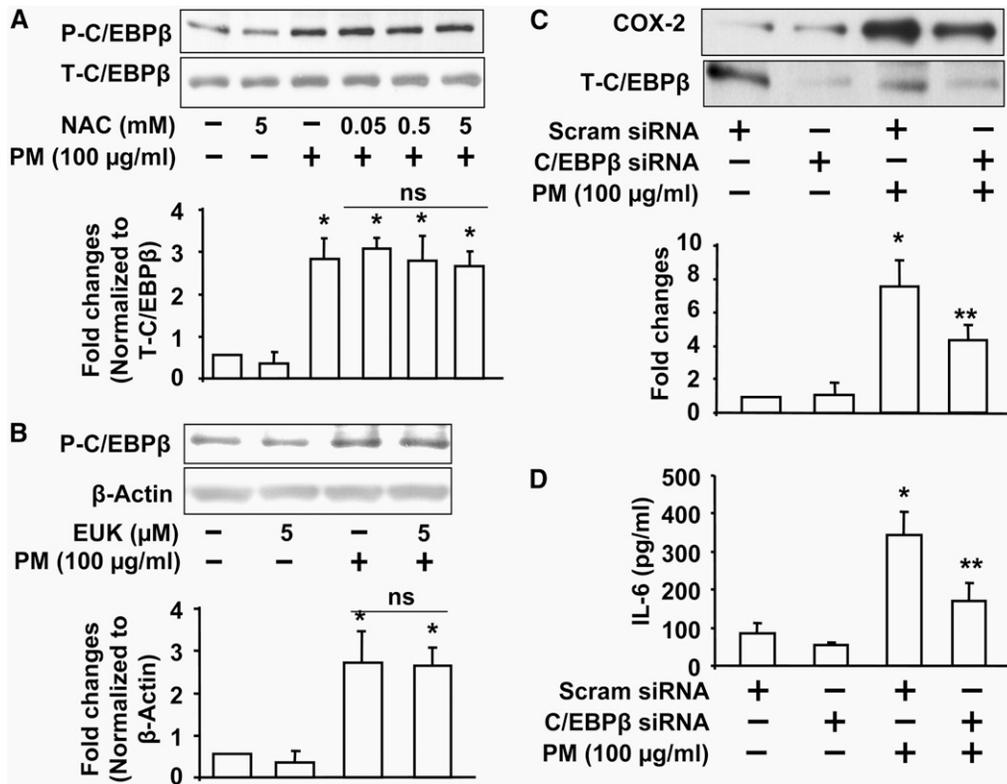
to a standard PM, SRM 1648, also increased ROS production, COX-2 expression, PGE2 release, IkB phosphorylation, and IL-6 release (data not shown). These earlier studies and our present results demonstrate the ability of different sources of PM to stimulate IL-6 in immortalized and primary cultures of HBEpCs, *in vitro*.

Expression of the IL-6 gene is regulated by binding of a number of transcription factors, including NF-κB, CREB, AP-1, and NF–IL-6 (C/EBP), to the 5′ region of the IL-6 gene (17). Transcriptional regulation of the IL-6 gene could be stimulus and/or cell specific, and activation of NF-κB has been

Figure 9. C/EBPβ regulates Baltimore PM–induced COX-2 expression and IL-6 secretion via ROS-independent pathway. In *A* and *B*, HBEpCs grown on 35-mm dishes to approximately 90% confluence were pretreated with varying concentrations of NAC (0.05, 0.5, and 5 mM) or EUK-134 (5 μM) for 1 hour. Cells were challenged with vehicle or vehicle plus Baltimore PM (100 μg/ml) for 15 minutes, and cell lysates (20 μg proteins) were subjected to SDS-PAGE and Western blotted with anti–phospho-C/EBPβ or C/EBPβ antibodies. Shown are representative blots and quantitative analyses from three independent experiments (mean ± SD). *$P <$ 0.05 versus vehicle. In *C*, HBEpCs grown on 35-mm dishes to approximately 50% confluence were transfected with scrambled siRNA or C/EBPβ siRNA (100 nM) for 72 hours. Cells were challenged with vehicle or vehicle plus Baltimore PM (100 μg/ml) for 24 hours, and cell lysates (20 μg proteins) were subjected to SDS-PAGE and Western blotted with anti–COX-2 or C/EBPβ antibodies as described in MATERIALS AND METHODS. Shown are representative blots and quantitative analyses from three independent experiments (mean ± SD). *$P <$ 0.05 versus vehicle; **$P <$ 0.05 versus PM challenge. In *D*, media from *C* were analyzed for IL-6 by ELISA. Values are mean ± SD from three independent experiments. *Significantly different from vehicle-challenged cells ($P <$ 0.05); **significantly different from cells challenged with Baltimore PM ($P <$ 0.01).
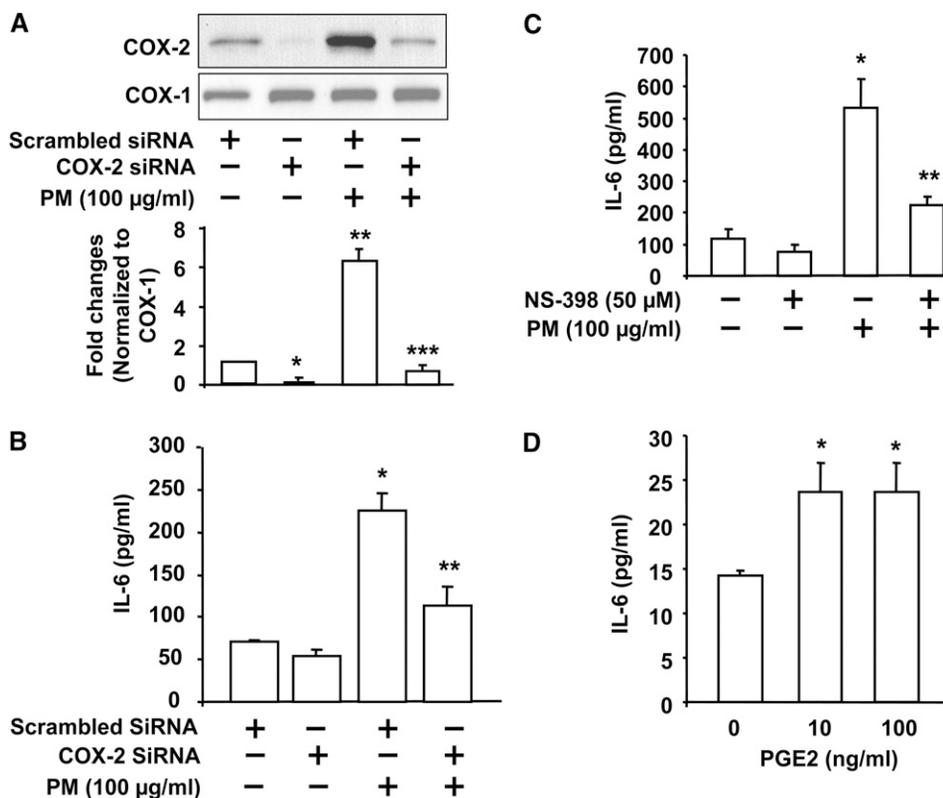
Figure 10. Involvement of COX-2 and PGE2 in Baltimore PM–induced IL-6 secretion. In *A* and *B*, HBEpCs grown on 35-mm dishes to approximately 50% confluence were transfected with scrambled siRNA (50 nM) or COX-2 siRNA (50 nM) for 72 hours before challenge with vehicle or vehicle plus Baltimore PM (100 μg/ml) for 24 hours. In *A*, cell lysates (20 μg proteins) were subjected to SDS-PAGE, and Western blotted with anti–COX-2 or –COX-1 antibodies. Shown are representative blots and quantitative analyses from three independent experiments. * and ** significantly different from scrambled siRNA-transfected cells exposed to vehicle ($P <$ 0.01); *** significantly different from COX-2 siRNA-transfected cells exposed to PM ($P <$ 0.01). In *B*, media from *A* were collected and analyzed for IL-6 by ELISA. Values are mean ± SD from three independent experiments. *Significantly different from scrambled siRNA-transfected cells exposed to vehicle ($P <$ 0.01); **significantly different from scrambled siRNA-transfected cells exposed to Baltimore PM ($P <$ 0.01). In *C*, HBEpCs grown to approximately 90% confluence were pretreated with COX-2 inhibitor, NS-398 (50 μM) for 1 hour, cells were challenged with vehicle or vehicle plus Baltimore PM (100 μg/ml) for 24 hours, and media were analyzed for IL-6 by ELISA. Values are mean ± SD from three independent experiments. *Significantly different from cells challenged with vehicle ($P <$ 0.05); **significantly different from cells exposed to Baltimore PM ($P <$ 0.01). In *D*, PGE2 (10, and 100 ng/ml) was added to HBEpCs grown on 35-mm dishes for 6 hours, media were collected, and analyzed for IL-6 by ELISA. Values are mean ± SD from three independent experiments. *Significantly different from cells exposed to vehicle ($P <$ 0.05).
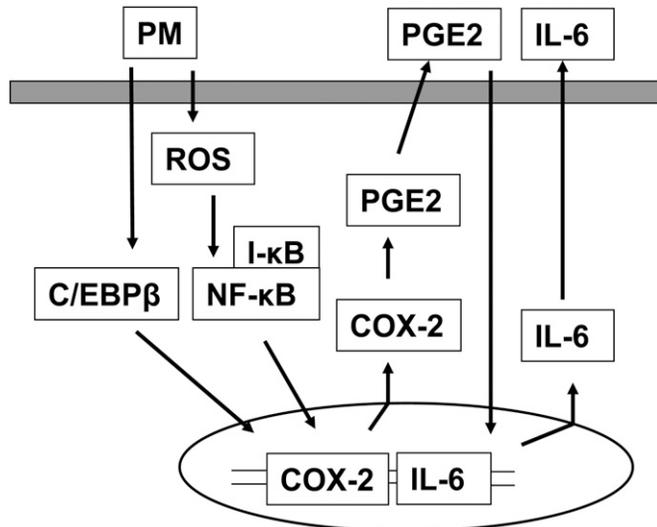
Figure 11. Proposed signaling pathways of ROS-dependent and -independent activation of COX-2 in PM-induced IL-6 secretion in HBEpCs. Exposure of epithelium to PM results in ROS generation and activation of NF-κB, which regulates COX-2 and IL-6 secretion. PM-induced expression of COX-2 enhances PGE2 that stimulates IL-6 in HBEpCs. Independent of ROS generation, PM also stimulates COX-2 expression via C/EBPβ signaling. These results suggest multiple pathways involved in ambient PM–mediated IL-6 generation in airway epithelium, which involve ROS-dependent and -independent activation of COX-2 and PGE2 signal transduction.

PGE2 to HBEpCs resulted in enhanced IL-6 production suggesting a role for PM-induced secretion of PGE2 in ROS-dependent and ROS-independent release of IL-6. Our results show that at 10 μg/ml of PM exposure, there was no significant increase in COX-2 expression (Figure 3) and phosphorylation of IkB (Figure 7). Although PM (10 μg/ml)-induced generation of ROS (Figure 4B) and IL-6 production (Figure 2A) are statistically significant, the changes are much smaller compared with exposure of cells to 100 μg/ml of PM (Figures 2 and 4). As ROS production via the mitochondrial electron transport system is upstream of NF-κB and COX-2 pathways, some of the observed effects of varying PM concentrations may be due to the downstream signaling involved in IL-6 production. While the ability of the coarse PM fraction and incinerator fly ash to induce the expression of COX-2 has been described earlier (17, 49), we report for the first time an ROS-dependent expression of COX-2 via NF-κB and ROS-independent activation of COX-2 via C/EBPβ by PM in HBEpCs. Although the mechanism(s) of PGE2-induced IL-6 release was not investigated in HBEpCs, addition of PGE2 stimulated IL-6 production via PGE2 receptors EP-2/4 linked to adenylate cyclase in BEAS-2B cell line (T59). A role for nickel, a component of PM also present in Baltimore PM, was demonstrated in Toll-like receptor-2–dependent chemokines released from human lung fibroblasts through a COX-2–mediated pathway (61). Nickel has been linked to human cardiac dysfunction and daily deaths in response to inhalation of fine PM (62). Future studies in murine models of asthma and cardiac hypertrophy will address the role of metal ions such as nickel and vanadium in ROS generation, COX-2 expression, PGE2 release, and IL-6 secretion in the airway and lung, which could contribute to the cardiopulmonary dysfunctions associated with inhalation of PM. Instillation of Baltimore PM to mice induced airway inflammation, increased influx of activated PMNs and eosinophils in alveolar space, and

stimulated IL-6 secretion in BAL fluid (data not shown) indicating the utility of this model for *in vivo* studies related to PM inhalation, ROS generation, and lung inflammation.

The present study has identified that PM-mediated activation of the transcriptional factor, C/EBPβ, regulates ROS-independent activation of COX-2 in HBEpCs. Several proinflammatory mediators stimulate COX-2 expression via C/EBPβ, and recently lysophosphatidic acid–mediated transactivation of EGF-R was shown to regulate COX-2 expression and PGE2 release via C/EBPβ in HBEpCs (63). Interestingly, recent studies show up-regulation of several EGF-R ligands in 16HBE14o airway epithelial cells exposed to PM with an aerodynamic diameter less than 2.5 μm (64). Intratracheal instillation of ROFA into perfused rabbit lungs activated EGF-R and mediated pulmonary vasoconstriction (65), and Zn^{2+}, also present in Baltimore PM, induced EGF-R activation and signaling in A431 cells (66). It is hypothesized that activation of C/EBPβ by PM might involve activation of EGF-R either by EGF-ligands and/or transactivation mechanism(s) involving G protein–coupled receptors in HBEpCs and which are currently under investigation.

Epidemiologic studies suggest an association between acute exposure to PM and increased hospitalization of patients with cardiovascular events (1–4). Exposure of normal individuals and people with cardiovascular disease to PM increases serum levels of IL-6 and C-reactive protein (22), which are independently associated with increased incidence of cardiovascular disease (23–26). These PM effects on humans have been partly supported by studies in murine models, which suggest that exposure to PM can modulate IL-6 production by alveolar macrophages and lead to reduced clotting times, intravascular thrombin formation, and accelerated arterial thrombosis (19). Therefore, PM-induced IL-6 generation, either independently or in association with other mediators, may be responsible for the development of cardiovascular events. As ROS play a key role in the development of cardiovascular diseases (67), and regulate COX-2 expression, PGE2 release, and IL-6 production in HBEpCs and other cell types, the targeting of excess ROS generation may represent a reasonable approach to alleviate PM-induced cardiopulmonary complications and reduce hospitalizations. The relationship between the doses used in the present studies and *in vivo* dose levels is difficult to accurately determine, but were, as indicated, many fold higher than those experienced in the Baltimore environment. While it is possible that variation in pathway activities may differ somewhat at lower concentrations, the present data identify PM-responsive targets within respiratory epithelial cells that may play crucial modulatory roles in respiratory signaling.

In summary, this study demonstrates ROS-dependent and ROS-independent stimulation of COX-2 expression, PGE2 release, and IL-6 secretion by PM in primary HBEpCs. While ROS-dependent activation of NF-κB regulates IL-6 secretion independent of COX-2, enhanced COX-2 expression by ROS resulted in PGE2 release, which also triggered IL-6. Further, ROS-independent activation of COX-2 was mediated by activation of the transcriptional factor C/EBPβ, with subsequent release of IL-6 via PGE2 signaling. We also show that the mitochondrial electron transport chain, but not NADPH oxidase, regulates PM-induced ROS production in HBEpCs. These novel ROS-dependent and ROS-independent pathways that regulate COX-2 expression, PGE2 release, and IL-6 secretion present potential targets to minimize the pro-inflammatory responses and cardiopulmonary events associated with inhalation of environmental air pollutants.

References

1. Oberdorster G, Gelein RM, Ferin J, Weiss B. Association of particulate air pollution and acute mortality: involvement of ultrafine particles? *Inhal Toxicol* 1995;7:111–124.

2. Samet JM, Dominici F, Curriero FC, Coursac I, Zeger SL. Fine particulate air pollution and mortality in 20 US cities, 1987–1994. *N Engl J Med* 2000;343:1742–1749.

3. Dominici F, McDermott A, Zeger SL, Samet JM. Airborne particulate matter and mortality: timescale effects in four US cities. *Am J Epidemiol* 2003;157:1055–1065.

4. Samet JM, Krewski D. Health effects associated with exposure to ambient air pollution. *J Toxicol Environ Health A* 2007;70:227–242.

5. Sandstrom T. Respiratory effects of air pollutants: experimental studies in humans. *Eur Respir J* 1995;8:976–995.

6. Dreher KL, Jaskot RH, Lehmann JR, Richards JH, McGee JK, Ghio AJ, Costa DL. Soluble transition metals mediate residual oil fly ash induced acute lung injury. *J Toxicol Environ Health* 1997;50:285–305.

7. Gonzalez-Flecha B. Oxidant mechanisms in response to ambient air particles. *Mol Aspects Med* 2004;25:169–182.

8. Schlesinger RB. The health impact of common inorganic components of fine particulate matter (PM2.5) in ambient air: a critical review. *Inhal Toxicol* 2007;19:811–832.

9. Becker S, Dailey LA, Soukup JM, Grambow SC, Devlin RB, Huang YC. Seasonal variations in air pollution particle-induced inflammatory mediator release and oxidative stress. *Environ Health Perspect* 2005; 113:1032–1038.

10. Franklin M, Zeka A, Schwartz J. Association between PM2.5 and all-cause and specific-cause mortality in 27 US communities. *J Expo Sci Environ Epidemiol* 2007;17:279–287.

11. Handzel ZT. Effects of environmental pollutants on airways, allergic inflammation, and the immune response. *Rev Environ Health* 2000;15: 325–336.

12. Peden DB. Air pollution in asthma: effect of pollutants on airway inflammation. *Ann Allergy Asthma Immunol* 2001;87:12–17.

13. Tao F, Gonzalez-Flecha B, Kobzik L. Reactive oxygen species in pulmonary inflammation by ambient particulates. *Free Radic Biol Med* 2003; 35:327–340.

14. Quay JL, Reed W, Samet J, Devlin RB. Air pollution particles induce IL-6 gene expression in human airway epithelial cells via NF-kappaB activation. *Am J Respir Cell Mol Biol* 1998;19:98–106.

15. Fujii T, Hayashi S, Hogg JC, Vincent R, Van Eeden SF. Particulate matter induces cytokine expression in human bronchial epithelial cells. *Am J Respir Cell Mol Biol* 2001;25:265–271.

16. Yu M, Zheng X, Witschi H, Pinkerton KE. The role of interleukin-6 in pulmonary inflammation and injury induced by exposure to environmental air pollutants. *Toxicol Sci* 2002;68:488–497.

17. Becker S, Mundandhara S, Devlin RB, Madden M. Regulation of cytokine production in human alveolar macrophages and airway epithelial cells in response to ambient air pollution particles: Further mechanistic studies. *Toxicol Appl Pharmacol* 2005;207:269–275.

18. Dagher Z, Garcon G, Billet S, Gosset P, Ledoux F, Courcot D, Aboukais A, Shirali P. Activation of different pathways of apoptosis by air pollution particulate matter (PM2.5) in human epithelial lung cells (L132) in culture. *Toxicology* 2006;225:12–24.

19. Mutlu GM, Green D, Bellmeyer A, Baker CM, Burgess Z, Rajamannan N, Christman JW, Foiles N, Kamp DW, Ghio AJ, *et al.* Ambient particulate matter accelerates coagulation via an IL-6-dependent pathway. *J Clin Invest* 2007;117:2952–2961.

20. Watterson TL, Sorensen J, Martin R, Coulombe RA Jr. Effects of PM2.5 collected from Cache Valley Utah on genes associated with the inflammatory response in human lung cells. *J Toxicol Environ Health* 2007;70:1731–1744.

21. Porter M, Karp M, Killedar S, Bauer SM, Guo J, Williams D, Breysse P, Georas SN, Williams MA. Diesel-enriched particulate matter functionally activates human dendritic cells. *Am J Respir Cell Mol Biol* 2007;37:706–719.

22. Ruckerl R, Ibald-Mulli A, Koenig W, Schneider A, Woelke G, Cyrys J, Heinrich J, Marder V, Frampton M, Wichmann HE, *et al.* Air pollution and markers of inflammation and coagulation in patients with coronary heart disease. *Am J Respir Crit Care Med* 2006;173:432–441.

23. Tracy RP. Epidemiological evidence for inflammation in cardiovascular disease. *Thromb Haemost* 1999;82:826–831.

24. Yudkin JS, Stehouwer CD, Emeis JJ, Coppack SW. C-reactive protein in healthy subjects: associations with obesity, insulin resistance, and endothelial dysfunction: a potential role for cytokines originating from adipose tissue? *Arterioscler Thromb Vasc Biol* 1999;19:972–978.

25. Harris TB, Ferrucci L, Tracy RP, Corti MC, Wacholder S, Ettinger WH Jr, Heimovitz H, Cohen HJ, Wallace R. Associations of elevated interleukin-6 and C-reactive protein levels with mortality in the elderly. *Am J Med* 1999;106:506–512.

26. Yeh ET. CRP as a mediator of disease. *Circulation* 2004;109:II11–II14.

27. Park CS, Chung SW, Ki SY, Lim GI, Uh ST, Kim YH, Choi DI, Park JS, Lee DW, Kitaichi M. Increased levels of interleukin-6 are associated with lymphocytosis in bronchoalveolar lavage fluids of idiopathic nonspecific interstitial pneumonia. *Am J Respir Crit Care Med* 2000; 162:1162–1168.

28. Inoue K, Takano H, Yanagisawa R, Sakurai M, Shimada A, Morita T, Sato M, Yoshino S, Yoshikawa T. Role of interleukin-6 in toll-like receptor 4 and 2 expressions induced by lipopolysaccharide in the lung. *Immunopharmacol Immunotoxicol* 2007;29:63–68.

29. Arcangeli G, Cupelli V, Giuliano G. Effects of silica on human lung fibroblast in culture. *Sci Total Environ* 2001;270:135–139.

30. Bankey PE, Williams JG, Guice KS, Taylor SN. Interleukin-6 production after thermal injury: evidence for nonmacrophage sources in the lung and liver. *Surgery* 1995;118:431–438. (discussion 438–439).

31. Frampton MW, Ghio AJ, Samet JM, Carson JL, Carter JD, Devlin RB. Effects of aqueous extracts of PM(10) filters from the Utah valley on human airway epithelial cells. *Am J Physiol* 1999;277:L960–L967.

32. Koyama S, Sato E, Nomura H, Kubo K, Miura M, Yamashita T, Nagai S, Izumi T. Bradykinin stimulates type II alveolar cells to release neutrophil and monocyte chemotactic activity and inflammatory cytokines. *Am J Pathol* 1998;153:1885–1893.

33. Mosmann TR, Sad S. The expanding universe of T-cell subsets: Th1, Th2 and more. *Immunol Today* 1996;17:138–146.

34. Yu M, Pinkerton KE, Witschi H. Short-term exposure to aged and diluted sidestream cigarette smoke enhances ozone-induced lung injury in B6C3F1 mice. *Toxicol Sci* 2002;65:99–106.

35. Grassl C, Luckow B, Schlondorff D, Dendorfer U. Transcriptional regulation of the interleukin-6 gene in mesangial cells. *J Am Soc Nephrol* 1999;10:1466–1477.

36. Matsusaka T, Fujikawa K, Nishio Y, Mukaida N, Matsushima K, Kishimoto T, Akira S. Transcription factors NF-IL6 and NF-kappa B synergistically activate transcription of the inflammatory cytokines, interleukin 6 and interleukin 8. *Proc Natl Acad Sci USA* 1993;90: 10193–10197.

37. Shukla A, Timblin C, BeruBe K, Gordon T, McKinney W, Driscoll K, Vacek P, Mossman BT. Inhaled particulate matter causes expression of nuclear factor (NF)-κB-related genes and oxidant-dependent NF-κB activation in vitro. *Am J Respir Cell Mol Biol* 2000;23:182–187.

38. Nam HY, Choi BH, Lee JY, Lee SG, Kim YH, Lee KH, Yoon HK, Song JS, Kim HJ, Lim Y. The role of nitric oxide in the particulate matter (PM2.5)-induced NFkappaB activation in lung epithelial cells. *Toxicol Lett* 2004;148:95–102.

39. Roberts JW, Budd WT, Ruvy MG, Camann DE, Fortmann RC, Lewis RG, Wallace LA, Spittler TM. Human exposure to pollutants in the floor dust of homes and offices. *J Expo Anal Environ Epidemiol* 1992; 2:127–146.

40. Walters DM, Breysse PN, Schofield B, Wills-Karp M. Complement factor 3 mediates particulate matter-induced airway hyperresponsiveness. *Am J Respir Cell Mol Biol* 2002;27:413–418.

41. Walters DM, Breysee PN, Wills-Karp M. Ambient urban Baltimore particulate-induced airway hyperresponsiveness and inflammation in mice. *Am J Respir Crit Care Med* 2001;164:1438–1443.

42. Saatian B, Yu XY, Lane AP, Doyle T, Casolaro V, Spannhake EW. Expression of genes for B7–H3 and other T cell ligands by nasal epithelial cells during differentiation and activation. *Am J Physiol Lung Cell Mol Physiol* 2004;287:217–225.

43. Bernacki SH, Nelson A, Abdullah L, Sheehan JK, Harris A, Davis CW, Randell SH. Mucin gene expression during differentiation of human airway epithelia in vitro. Muc4 and muc5b are strongly induced. *Am J Respir Cell Mol Biol* 1999;20:595–604.

44. Zhao Y, He D, Saatian B, Watkins T, Spannhake EWm, Pyne NJ, Natarajan V. Regulation of lysophosphatidic acid-induced epidermal growth factor receptor transactivation and interleukin-8 secretion in human bronchial epithelial cells by protein kinase Cδ, lyn kinase, and matrix metalloproteinases. *J Biol Chem* 2006;281:19501–19511.

45. Usatyuk PV, Parinandi NL, Natarajan V. Redox regulation of 4-hydroxy-2-nonenal-mediated endothelial barrier dysfunction by focal adhesion, adherens, and tight junction proteins. *J Biol Chem* 2006;281: 35554–35566.

46. Usatyuk PV, Romer LH, He D, Parinandi NL, Kleinberg ME, Zhan S, Jacobson JR, Dudek SM, Pendyala S, Garica JGN, *et al.* Regulation

of hyperoxia-induced NADPH oxidase activation in human lung endothelial cells by the actin cytoskeleton and cortactin. *J Biol Chem* 2007;282:23284–23295.

47. Mukhopadhyay P, Rajesh M, Hasko G, Hawkins BJ, Madesh M, Pacher P. Simultaneous detection of apoptosis and mitochondrial superoxide production in live cells by flow cytometry and confocal microscopy. *Nat Protocols* 2007;2:2295–2301.

48. Samet JM, Ghio AJ, Costa DL, Madden MC. Increased expression of cyclooxygenase 2 mediates oil fly ash-induced lung injury. *Exp Lung Res* 2000;26:57–69.

49. Fritsch S, Diabate S, Krug HF. Incinerator fly ash provokes alteration of redox equilibrium and liberation of arachidonic acid in vitro. *Biol Chem* 2006;387:1421–1428.

50. Huang YT, Soukup J, Harder S, Becker S. Mitochondrial oxidant production by a pollutant dust and NO-mediated apoptosis in human alveolar macrophage. *Am J Physiol Cell Physiol* 2003;284:C24–C32.

51. Li N, Ragheb K, Lawler G, Sturgis J, Rajwa B, Melendez JA, Robinson JP. Mitochondrial complex I inhibitor rotenone induces apoptosis through enhancing mitochondrial reactive oxygen species production. *J Biol Chem* 2003;278:8516–8525.

52. Lee JY, Jung GY, Heo HJ, Yun MR, Park JY, Bae SS, Hong KW, Lee WS, Kim CD. 4-Hydroxynonenal induces vascular smooth muscle cell apoptosis through mitochondrial generation of reactive oxygen species. *Toxicol Lett* 2006;166:212–221.

53. Cheng DS, Han W, Chen SM, Sherrill TP, Chont M, Park GY, Sheller JR, Plosukhin VV, Christman JW, Yull FE, *et al.* E3 ubiquitin ligase Cblb regulates the acute inflammatory response underlying lung injury. *Nat Med* 2007;13:920–926.

54. Park GY, Christman JW. Nuclear factor kappa B is a promising therapeutic target in inflammatory lung disease. *Curr Drug Targets* 2006;7:661–668.

55. Becker S, Fenton MJ, Soukup JM. Involvement of microbial components and toll-like receptors 2 and 4 in cytokine responses to air pollution particles. *Am J Respir Cell Mol Biol* 2002;27:611–618.

56. Fujii T, Hayashi S, Hogg JC, Mukae H, Suwa T, Goto Y, Vincent R, van Eden SF. Interaction of alveolar macrophages and airway epithelial cells following exposure to particulate matter produces mediators that stimulate the bone marrow. *Am J Respir Cell Mol Biol* 2002;27:34–41.

57. Becker S, Soukup JM, Gallagher JE. Differential particulate air pollution induced oxidant stress in human granulocytes, monocytes and alveolar macrophages. *Toxicol In Vitro* 2002;16:209–218.

58. Xia T, Korge P, Weiss JN, Li N, Venkatesen MI, Sioutas C, Nel A. Quinones and aromatic chemical compounds in particulate matter induce mitochondrial dysfunction: implications for ultrafine particle toxicity. *Environ Health Perspect* 2004;112:1347–1358.

59. Soberanes S, Panduri V, Mutlu GM, Ghio A, Bundinger GR, Kamp DW. p53 mediates particulate matter-induced alveolar epithelial cell mitochondria-regulated apoptosis. *Am J Respir Crit Care Med* 2006; 174:1229–1238.

60. Dye JA, Adler KB, Richards JH, Dreher KL. Role of soluble metals in oil fly ash-induced airway epithelial injury and cytokine gene expression. *Am J Physiol* 1999;277:L498–L510.

61. Brant KA, Fabisiak JP. Nickel alteration of TLR2-dependent chemokine profiles in lung fibroblasts are mediated by COX-2. *Am J Respir Cell Mol Biol* 2008;38:591–599.

62. Laden F, Neas LM, Dockery DW, Schwartz J. Association of fine particulate matter from different sources with daily mortality in six US cities. *Environ Health Perspect* 2000;108:941–947.

63. He D, Natarajan V, Stern R, Gorshkova IA, Solway J, Spannhake EWm, Zhao Y. Lysophosphatidic acid-induced transactivation of epidermal growth factor receptor regulates cyclooxygenase-2 expression and prostaglandin E2 release via C/EBPβ in human bronchial epithelial cells. *Biochem J* 2008;412:153–162.

64. Rumelhard M, Ramgolam K, Hamel R, Marono F, Baeza-Squiban A. Expression and role of EGFR ligands induced in airway cells by PM2.5 and its components. *Eur Respir J* 2007;30:1064–1073.

65. Huang YC, Wu W, Ghio AJ, Carter JD, Silbajoris R, Devlin RB, Samet JM. Activation of EGF receptors mediates pulmonary vasoconstriction induced by residual oil fly ash. *Exp Lung Res* 2002;28:19–38.

66. Samet JM, Dewar BJ, Wu W, Graves LM. Mechanisms of Zn(2+)-induced signal initiation through the epidermal growth factor receptor. *Toxicol Appl Pharmacol* 2003;191:86–93.

67. Shah AM, Channon KM. Free radicals and redox signaling in cardiovascular disease. *Heart* 2004;90:486–487.